

## Development of Melting System for Measurement of Trace Elements and Ions in Ice Core

Sang-Bum Hong,<sup>†,\*</sup> Khanghyun Lee,<sup>†</sup> Soon-Do Hur,<sup>†</sup> Sungmin Hong,<sup>‡</sup> Tseren-Ochir Soyol-Erdene,<sup>†,¶</sup> Sun-Mee Kim,<sup>†,||</sup> Ji-Woong Chung,<sup>†</sup> Seong-Joon Jun,<sup>†</sup> and Chang-Hee Kang<sup>§</sup>

<sup>†</sup>Korea Polar Research Institute, KIOST, Incheon 406-840, Korea. \*E-mail: hong909@kopri.re.kr

<sup>‡</sup>Department of Ocean Sciences, Inha University, Incheon 402-751, Korea

<sup>§</sup>Department of Chemistry and Research Institute for Basic Sciences, Jeju National University, Jeju-si 690-756, Korea

Received August 13, 2014, Accepted December 16, 2014, Published online March 23, 2015

We present a titanium (Ti) melting head divided into three zones as an improved melting system for decontaminating ice-core samples. This system was subjected to performance tests using short ice-core samples (4 × 4 cm<sup>2</sup>, ~5 cm long). The procedural blanks (PBs) and detection limits of ionic species, with the exception of NO<sub>3</sub><sup>-</sup>, were comparable with published values, but for elements the experimental procedures should be refined to obtain valid Zn concentrations due to the PB of ~90.0 ± 16.2 ng/L. The improved melting system efficiently decontaminated the samples, as verified by the concentration profiles of elements and ions in the melted samples from the three melting-head zones. The recovery of trace elements in ice-core samples was ~70–120% at ~100 ng/L in artificial ice cores. Because of the memory effects between ice-core samples melted in series, the melting system should be rinsed at least 5–6 times (in a total volume of ~2.5 mL deionized water) after each melting procedure. Finally, as an application of this technique, trace elements were measured in ice-core samples recovered from the East Rongbuk Glacier, Mount Everest, (28°03'N, 86°96'E, 6518 m a.s.l.), and the concentrations of trace elements following mechanical chiseling and the melting method were compared.

**Keywords:** Ice core, Melting system, Performance tests, Titanium melting head

### Introduction

Ice cores from polar and high-alpine regions contain various chemical proxy records in terms of past atmospheric composition. Acquisition of these proxy parameters has been recognized as a unique means of obtaining environmental records related to natural phenomena such as climate and volcanism and human activities. However, such studies have proved difficult to perform, mainly due to the low concentrations of the chemical components to be measured. Ice cores easily become contaminated in the course of the process from drilling to handling, so it is necessary to remove the possibly contaminated outer parts of the samples without transferring the contamination to the central parts and to check the efficiency of the procedure to ensure data reliability.<sup>1–3</sup>

Ice-core decontamination involves the removal of contaminants in the outer layers of the core. Conventional procedures involve manual methods such as mechanical decontamination using stainless steel chisels or knives or the removal of contamination by successively washing the samples with

ultrapure water.<sup>4–6</sup> The advantages of these methods are minimal interference among samples, flexible extraction time, and stable instrumental analysis. The disadvantages include time-consuming work due to strict and complicated procedures, relatively low-resolution proxy records, and difficulty in using online measurement systems.

An ice-core melting system was developed as an alternative to manual decontamination methods in the early 1990s in response to the need for continuous and high-resolution proxy records, particularly for areas with low accumulation rates or glaciers with pronounced layer thinning.<sup>7</sup> This decontamination method has higher preparation efficiency and can be applied to an online measurement system. Despite much simpler sample preparation steps than with conventional methods, however, unresolved drawbacks of the melting system include errors in the measurement of the elements comprising the melting head, the possibility of cross-contamination between samples that are melted in series, and unstable instrumental analysis due to the short extraction time.<sup>7–14</sup>

In previous studies, the melting heads of the melting system have been constructed with Teflon-coated metals such as Al,<sup>7–9,11</sup> Ni-plated brass,<sup>10</sup> Ni-270,<sup>12</sup> and Au.<sup>13,14</sup> The geometry of the melting surface has been carefully designed to reduce the risk of meltwater crossover from the external to the internal part. The implications of using a melting head made of titanium (Ti) have not been explored in previous work, although this method has some advantages. In

¶ Present address: Department of Environmental Sciences and Chemical Engineering, National University of Mongolia, Ulaanbaatar 14201, Mongolia.

|| Present address: Environmental Certification Department, Korea Environmental Industry & Technology Institute (KEITI), 215 Jinheungno, Eunpyeong-gu 122-706, Seoul, Korea

particular, it was reported that the use of a Ti melting head might allow meaningful measurement of trace amounts of Ni, Cu, and Zn.<sup>10</sup>

The efficiency of decontamination procedures using a melting system needs to be firmly established to ascertain that the melted samples from the inner part of an ice core are free from the contaminants in its outer part. Performance tests of melting systems have not been systematically conducted in previous works.<sup>7–14</sup> However, the decontamination and the recovery efficiencies of selected chemicals in ice cores processed by the melting system must be carefully investigated because the original and unaltered levels encoded in the ice core must be determined. The chemical components of the melted sample from the ice core can be adsorbed onto the surfaces of the melting head and connecting tubes and can also remain there depending on the materials comprising the melting system. As a result, they should be removed to minimize interference between samples.

Here we report an improved melting system using a Ti melting head that can be used to analyze trace elements and ionic species in high-alpine ice cores. Performance tests such as decontamination efficiency, recovery efficiency, and memory effects of the melting system were systematically performed using an artificial ice core. We present the results of comparing trace element concentrations obtained with the chiseling method and melting method using a high-altitude ice core from Mount Everest.

## Experimental

**Melting System.** The ice-core melting apparatus (Figures 1 and 2 and Table 1) consists of an ice-core sample holder (ISH) frame, a melting head (MH), a Teflon-coated Al (Al alloy-6061) heating body (HB), a heating cartridge (HC), and a peristaltic pump (PP). All these items, except PP, are installed in a freezer (static type, temperature  $-10$  to  $-15$  °C) in a laminar-flow hood (class 100) with a high-efficiency particulate air (HEPA) filter.

An ISH made of polytetrafluoroethylene (PTFE) was designed to align a short ice-core sample ( $4 \times 4$  cm<sup>2</sup>,  $\sim 5$  cm long) with the center of the melting head and minimize the contact area with the ice-core sample, thereby minimizing the possibility of contamination from the surface of the ISH. The circular Ti melting head ( $>99.99\%$  Ti) was divided into three zones. Titanium was chosen for the melting head because of the commercial availability in high purity and chemical stability, although the thermal conductivity (0.219 W/cm/K) of Ti is relatively low. Therefore, its interference with the levels of elements typically present in ice cores was expected to be very low. When an ice-core sample with a cross-sectional area of  $4 \times 4$  cm<sup>2</sup> was put on the melting head, which had an inner-zone diameter of 2.76 cm, contaminants in the outer part of the ice core did not affect the melted samples from the inner part because  $\sim 60\%$  of the sample volume was removed. Previous work has shown that 50% of the ice volume ( $\sim 30\%$  of

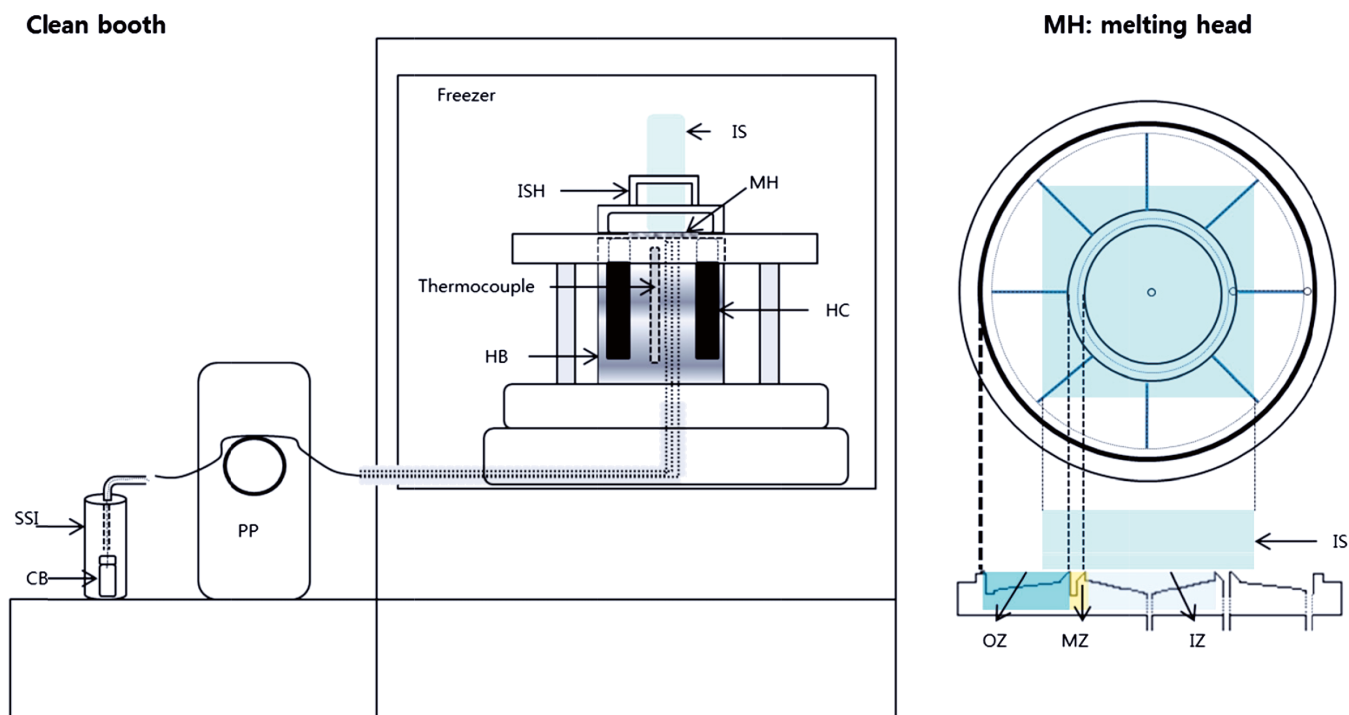


**Figure 1.** Melting system installed in a clean booth (class 100) and melting head [SSI: sample safety introduction part, CB: sample collection bottle, PP: peristaltic pump (Model IP65), IS: ice core sample, ISH: ice core sample holder frame, MH: melting head, HB: Al heating body, HC: Cu heating cartridge, IZ: inner zone of melting head (gray colored zone), MZ: middle zone of melting head (yellow colored zone), OZ: outer zone of melting head (blue colored zone), Groove: blue line in the OZ].

the initial core radius) must be removed to obtain a contamination-free ice-core melted sample.<sup>15</sup> The melting head was divided into three zones to examine the possibility that the melted sample from the inner part of the core might have mixed with that from the outer part during melting.

The melting-head surface was partially grooved, allowing the melted sample to drain efficiently from the melting head; without grooves, the surface tension of the melted sample would obstruct the flow of the melted solution. In particular, the melted sample of firm snow (density  $\sim 0.5\text{--}0.8\text{ g/cm}^3$ )

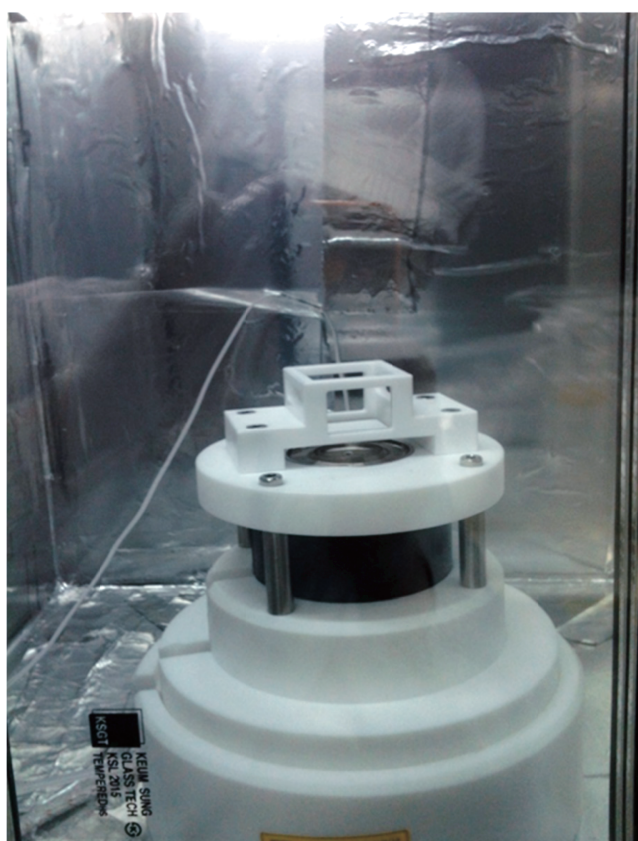


**Figure 2.** Melting system installed in freezer (Model LCT-110 F, Lassele Co. Ltd) under the clean booth (class 100).

can readily penetrate from the outer to the inner part because of the capillary force caused by the material's porosity.<sup>12</sup> In this study, however, grooves (width 0.5 mm, depth 0.5 mm) were constructed only in the outer layer of the head that affects the outer part of an ice core because the device was designed specifically for melting only ice-core samples. As a result, this design could preclude the adherence of insoluble impurities in the melted sample from the inner part of an ice core to the narrow slits in the inner layer of the melting head.

The HB of the melting head was made of aluminum (Alloy 6106, 2.37 W/cm/K) coated with Teflon (0.6  $\mu\text{m}$  thick). The Cu heating rods (4  $\times$  50 W) were put into holes in the Al heating body installed in a Teflon frame, and a thermocouple was positioned just under the center of the melting head. The melting-head temperature was controlled at 23–25  $^{\circ}\text{C}$ , and the melting rate of the ice-core sample was  $\sim 0.6\text{--}0.7\text{ cm/min}$ . The sides of the Teflon frame and the Al heating body were cut out so that the melting head connected to perfluoroalkoxy copolymer resin (PFA) tubes could be conveniently put on the Al heating body without causing contamination. This arrangement was also useful for maintaining the melting system during melting procedures (see Figure 2).

In this system, a melted sample passes through three Ti nozzles (length 11 mm, inner and middle zone inner diameter (i.d.) 1.5 mm, outer zone i.d. 2 mm) in the melting head, whose inner diameters were designed to prevent clogging of the insoluble impurities in the melted sample. The melted sample then drains out through PFA tubes (inner and middle zones i.d. 1.6 mm; outer zone i.d. 2.4 mm). These are directly connected to the Ti nozzles so that the melted samples cannot come into contact with the Al heating body, and they are insulated so that the melted sample in the PFA tubes does not refreeze. The PFA tubes extend out from the freezer and are directly connected to PTFE tubes (i.d. 1.1 mm) and TYGON E-Lab tubes (i.d. 2.5 mm for outer zone, 1.5 mm for middle zone, and 2.3 mm for inner zone) attached to a peristaltic pump head (ISMATEC, model IP65). The inner diameter of the TYGON E-Lab tubes was selected to ensure that lateral flow on the melting head would be strongly outward, in order to minimize contamination of the melted material from the inner zones by melted

**Table 1.** Specifications of the melting system.

	Description
Material	Melting head: titanium (>99.99%); heating body: Teflon-coated aluminum alloy 6106
Zone	Three layers: inner zone, middle zone, outer zone
Type	Concentric circle: inner zone i.d.: 27.6 mm, middle zone i.d.: 34.2 mm, outer zone i.d.: 59.8 mm
Surface	Inner and middle zone: flat surface, outer zone: flat surface with narrow slits (width: 0.5 mm)
Melting head temperature	$\sim 23^{\circ}\text{C}$
Heat source	200 W (50 W Cu cartridge four each)
Sample holder	Teflon frame
Cross sectional area of ice core	$4 \times 4\text{ cm}^2$
Melting rate	$\sim 0.6\text{--}0.7\text{ cm/min}$
Weight	60–100 g (rectangular solid made of LDPE)
Filter setup on the melting head	No setup

material from the outer part of the core. The melted material was collected in a sample-collection bottle (Nalgene, MA, USA, NA-2103-0001 for elements and WH. 986704 for ions) under safety sample introduction in order to prevent any inclusion of contaminants during sampling under clean-booth conditions (see Figure 1).<sup>16</sup> The inner surface of the freezer was also coated with an Al-foil-supported fluorinated ethylene-propylene (FEP) film (Saint-Gobain Company, BYTAC Type AF-21: #D1069329, Courbevoie, France) to protect the melted samples from contamination in the freezer itself.

Processing of ice-core samples was undertaken as follows. The whole ice core was cut off using a bandsaw (Rexon, BS-10KA, Taichung, Taiwan) inside a cold room at approximately  $-12\text{ }^{\circ}\text{C}$ . Operators wore clean garments (Dupont, Tyvek, USA) and disposable polyethylene gloves during cutting procedures. The bandsaw was fitted with carbon steel blades (Rexon, No. 96341, 6 mm wide), and impurities on the surface of the blade were removed by cutting a blank ice core before each sample. In addition, after cutting the ice core, the impurities on the ice-core pieces were removed using a stainless steel blade. Each sample was then packed in a polyethylene bag and stored in a freezer (approximately  $-20\text{ }^{\circ}\text{C}$ ) installed in a low-temperature laboratory. The ice-core samples for melting were put in an insulated ice box with ice packs and carried to a laminar-flow hood (class 100) where the melting system was installed. Before beginning the melting

procedure, the melting system was thoroughly washed out using ultrapure water (Millipore Milli-Q Element, Darmstadt, Germany, hereafter DW), and both a bottle blank and a system blank were regularly collected throughout the melting procedure. The operators wore clean garments (hair cap, boots, mask, and disposable polyethylene gloves) to minimize contamination during the operations. Details of the procedures used to clean the melting system and prepare artificial ice core are presented in Supporting Information.

**Analytical Procedures: Inductively Coupled Plasma Mass Spectrometry and Ion Chromatography System.** The instrumental conditions under which trace elements and ionic species in the melted sample were analyzed are summarized in Table 2. The inductively coupled plasma mass spectrometry (ICP-MS) system was installed in a clean laboratory (class 1000), and the ion chromatography (IC) system was installed in a class 10 laminar airflow booth in the same clean laboratory. Analytical procedures for the ICP-MS are described in detail elsewhere.<sup>17</sup> All samples for trace element determination were acidified to 1% with Fisher "Optima" grade ultrapure  $\text{HNO}_3$  (A467-250) in a class 10 laminar airflow booth in a clean laboratory (class 1000). All cation and anion species were analyzed using a two-channel IC system combining two Dionex IC sets (Sunnyvale, CA, USA). This system made it possible to simultaneously determine both cations and anions with reduced sample volume ( $\sim 3\text{ mL}$ ) and analysis

**Table 2.** Analytical conditions of inductively coupled plasma mass spectrometry (ICP-MS) and ion chromatography (IC) system for the analysis of trace elements and ions.

	Anion analysis	Cation analysis
System	ICS 2000	IC 2100
Column	IonPac AS 15 (2 × 250 mm)	IonPac CS 12A (4 × 250 mm)
Eluent	6–55 mM KOH (gradient)	20 mM MSA (isocratic)
Suppressor	ASRS-300	CSRS-300
Flow rate	0.5 mL/min	1.0 mL/min
Injection volume	500 $\mu\text{L}$	500 $\mu\text{L}$
Background conductivity	$\sim 0.640\text{ }\mu\text{S/cm}$	$\sim 0.065\text{ }\mu\text{S/cm}$
Background pressure	$\sim 2209\text{ psi}$	$\sim 2069\text{ psi}$
Element analysis		
System	ICP-MS (Perkin Elmer Sciex, ELAN 6100, MA, USA)	
Sampler and skimmer cone	Pt cone	
Spray chamber	Glass cyclonic spray chamber	
Nebulizer	Glass micromist nebulizer	
Injector	Quartz injector	
RF power	1150 W	
Nebulizer gas	0.91–0.93 L/min (daily optimized)	
Oxide levels (CeO/Ce)	$< 0.3\%$	
Scanning mode	Peak hopping	
Sweeps per reading	20	
Peading per replicate	1	
Number of replicates	3	
Dwell time per acquisition	50 ms	
Measuring time	90 s	
Sample uptake	1.2 mL/min	



time of ~25 min. Samples were loaded from an AS40 automated sampler (Dionex). A gradient elution was applied to analyze anions using potassium hydroxide (KOH), produced by an EG 50 system, as an eluent with a flow rate of 0.5 mL/min. The gradient was 6 mM KOH from 0 to 3.5 min, 6–55 mM KOH from 3.5 to 19.5 min, 55 mM KOH from 19.5 to 21.5 min, 55 to 6 mM KOH from 21.5 to 21.6 min, and 6 mM KOH from 21.6 to 25 min. Chromeleon 6.80 software (Dionex) was used for data acquisition and peak integration. Calibrations were conducted using multilevel standard solutions diluted with a stock solution from Dionex (anion P/N 057590, cation P/N 046070). For organic acids and methanesulfonic acid (MSA), standard solutions were prepared from their sodium salts to derive the calibration curves.<sup>18</sup>

Instrumental detection limits (IDLs) for the analyses of elements and ionic species are presented in Tables 3 and 4. The coefficients of variation (CVs) varied according to concentrations and were generally <5% for elements at high concentrations. The CV of ionic species varied from 1 to 10% at levels of 1–10 µg/L. The accuracy of measurement data was estimated by analyzing certified standard reference materials (SRMs) of artificial rainwater (BCR-408, Community Bureau of Reference, Geel, Belgium) for ionic species and of river water (SLRS-5, National Research Council Canada, Ottawa, Canada) for trace elements (Table S1).

## Results and Discussion

### Cleanliness of Laminar-Flow Hood, Sample Collection Bottles, and Melting System. Dust concentration in the clean

booth where the melting system was installed was periodically measured using a particle dust monitor (GT-521 particle counter, Met One Instruments). The concentration of dust particles with diameters of 0.3 and 0.5 µm was <~20 particles ft<sup>-3</sup>, which was fully satisfactory for ice-core sample melting operations. The dust concentration was measured 150 cm above the booth's base, a position roughly similar to the height of the melting head of the melting system installed in the laminar-flow hood.

The cleaning procedures for the sample collection bottles used for trace elements were previously well established, showing that the contributions of trace elements from the bottles are negligible.<sup>19,20</sup> We thus report only the cleanliness of sample collection bottles used for the ionic species investigated in this study. The bottle blanks (B-1), which were measured by injection of DW in sample collection bottles, were compared with the system blanks of the melting system (B-2), the instrumental blank, and the lowest level of calibration ranges (Figure 3). The results show that peaks of CH<sub>3</sub>CO<sub>2</sub><sup>-</sup>, HCO<sub>2</sub><sup>-</sup>, NO<sub>2</sub><sup>-</sup>, NO<sub>3</sub><sup>-</sup>, and NH<sub>4</sub><sup>+</sup> of B-1 are larger than those of other ionic species, which show no measurable peaks. In the B-2 case, CH<sub>3</sub>CO<sub>2</sub><sup>-</sup>, HCO<sub>2</sub><sup>-</sup>, NO<sub>2</sub><sup>-</sup>, NO<sub>3</sub><sup>-</sup>, and NH<sub>4</sub><sup>+</sup> peaks are clearer than the B-1 peaks, but no clear increments of other peaks are observed. This indicates that these species can be influenced by the cleanliness of the melting system and can affect its blank levels. Results for the instrumental blank were mainly related to the quality of the DW and showed measurable peaks for HCO<sub>2</sub><sup>-</sup>, NO<sub>2</sub><sup>-</sup>, and NH<sub>4</sub><sup>+</sup>. Thus, the CH<sub>3</sub>CO<sub>2</sub><sup>-</sup>, HCO<sub>2</sub><sup>-</sup>, NO<sub>2</sub><sup>-</sup>, NO<sub>3</sub><sup>-</sup>, and NH<sub>4</sub><sup>+</sup> peaks in the system blanks (B-2) can probably be ascribed to the combined effects of

**Table 3.** Intercomparisons of performances of melting systems for ionic species (unit: µg/L).

Species	Huber <i>et al.</i> <sup>9</sup>		Osterberg <i>et al.</i> <sup>12</sup>		Cole-Dai <i>et al.</i> <sup>23</sup>		Morganti <i>et al.</i> <sup>24</sup>	This study ( <i>n</i> > 5)		
	IDL <sup>a</sup>	PB <sup>b</sup>	IDL <sup>c</sup>	CMDS DL <sup>d</sup>	IDL	PB		IDL <sup>e</sup>	IDL <sup>f</sup>	PDL <sup>g</sup>
Na <sup>+</sup>	0.8	≤IDL	0.3	0.6	0.04	~0.2	0.09	0.02	0.68	0.21 ± 0.23
NH <sub>4</sub> <sup>+</sup>	1.4	≤IDL			0.06	~0.04	0.15	0.14	0.69	0.27 ± 0.23
K <sup>+</sup>	1.8	≤IDL	0.1	0.1	0.7	~0.7	0.13	0.16	<IDL	<IDL
Mg <sup>2+</sup>	1.1	≤IDL	0.06	0.1	0.004	~0.1	0.11	0.08	<IDL	<IDL
Ca <sup>2+</sup>	2.6	3.8 ± 1.2	0.3	2.0	0.004	~2	0.11	0.20	<IDL	<IDL
CH <sub>3</sub> CO <sub>2</sub> <sup>-</sup>	0.4	≤IDL						0.09	0.96	0.79 ± 0.32
HCO <sub>2</sub> <sup>-</sup>	0.3	≤IDL						0.08	0.59	0.54 ± 0.20
MSA	1.2	≤IDL	0.07	0.07			0.1	0.02	0.07	0.09 ± 0.02
Cl <sup>-</sup>	0.1	0.3 ± 0.1	0.3	0.7	0.4	~0.5	0.15	0.05	0.40	0.83 ± 0.13
SO <sub>4</sub> <sup>2-</sup>	1.0	6.4 ± 3.3	0.1	0.2	0.07	~0.1	0.08	0.02	0.36	0.62 ± 0.12
NO <sub>3</sub> <sup>-</sup>	0.5	≤IDL	0.2	0.9	0.02	~1.5	0.02	0.02	0.94	1.97 ± 0.31

<sup>a</sup> Instrumental detection limit (IDL) was defined as the amount of solute producing a signal-to-noise ratio of 3 (errors correspond to 1σ), instrument: ion chromatography (IC) system.

<sup>b</sup> Procedural blank (PB) was calculated as the average of 10 blank artificial cores after continuous melting and analysis.

<sup>c</sup> IDL was calculated by 3σ of 10 DI water samples, instrument: IC system.

<sup>d</sup> CMDS DL (the detection limit of continuous melting with a discrete sampling system) was calculated by 3σ of 10 DI water samples subjected to continuous melting with a discrete sampling (CMDS) system.

<sup>e</sup> IDL was calculated as 3σ of 10 replicates of a 1 µg/L<sup>-1</sup> (Na<sup>+</sup>, NH<sub>4</sub><sup>+</sup>, K<sup>+</sup>, Mg<sup>2+</sup>, Ca<sup>2+</sup>, MSA) or 2 µg/L<sup>-1</sup> (Cl<sup>-</sup>, NO<sub>3</sub><sup>-</sup>, SO<sub>4</sub><sup>2-</sup>) standard, instrument: IC system.

<sup>f</sup> IDL was calculated by 3σ of 10 DI water samples, instrument: IC system.

<sup>g</sup> Procedural detection limit (PDL) was calculated as 3σ of melted blank artificial ice cores using the melting system.

<sup>h</sup> PB was calculated as the average of melted blank artificial cores using the melting system (errors correspond to 1σ).

**Table 4.** Intercomparisons of performances of melting systems for trace elements (unit: ng/L).

Species	Knusel <i>et al.</i> <sup>11</sup>		Osterberg <i>et al.</i> <sup>12</sup>		This study ( $n > 5$ )		
	IDL <sup>a</sup>	PB <sup>b</sup>	IDL <sup>c</sup>	CMDS DL <sup>d</sup>	IDL <sup>e</sup>	PDL <sup>f</sup>	PB <sup>g</sup>
V			0.1	0.3	1.8	2.0	3.3 ± 1.5
Cr			0.14	0.76	12.0	14.1	<IDL
Mn	44	<IDL	1	21	2.5	2.5	3.6 ± 1.1
Co	2	2.5 ± 3.4	0.41	0.83	0.7	1.4	<IDL
Ni					2.7	2.7	5.2 ± 1.3
Cu			3.3	19.3	2.5	5.6	12.3 ± 3.7
Zn					5.9	15.4	90.0 ± 16.2
As					3.6	2.5	<IDL
Rb					0.6	0.9	<IDL
Sr	0.46	22 ± 3.2	0.3	0.7	0.2	0.6	2.4 ± 1.2
Cd			0.03	0.13	0.6	1.1	<IDL
Sb					0.4	1.7	4.8 ± 6.7
Pb			0.2	0.9	0.6	2.0	5.9 ± 2.9
Bi			0.03	0.08	0.1	0.2	1.2 ± 2.1

<sup>a</sup> Instrumental detection limit (IDL) was calculated using the German industry norm (Deutsche Industrie Norm, DIN) 32645, Instrument: inductively coupled plasma sector field mass spectrometry.

<sup>b</sup> Procedural blank (PB) was determined from blank ice-core sections by the continuous ice-core melting device (CIM) analysis (errors correspond to 1 $\sigma$ ).

<sup>c</sup> IDL was calculated by 3 $\sigma$  of 10 DI water samples, Instrument: inductively coupled plasma sector field mass spectrometry.

<sup>d</sup> CMDS DL (the detection limit of continuous melting with a discrete sampling system) was calculated by 3 $\sigma$  of 10 DI water samples subjected to continuous melting with a discrete sampling (CMDS) system.

<sup>e</sup> IDL was calculated by 3 $\sigma$  of 10 DI water samples, instrument: inductively coupled plasma mass spectrometry.

<sup>f</sup> Procedural detection limit (PDL) was calculated by 3 $\sigma$  of blank artificial ice core samples melted using melting system.

<sup>g</sup> PB were determined by preconcentration method (roughly 30 times) by non-boiling evaporation of melted blank ice core samples using melting system (~60 mL) (errors correspond to 1 $\sigma$ ).

DW quality and the cleanliness of sample collection bottles and of the melting system. Among these species, CH<sub>3</sub>CO<sub>2</sub><sup>-</sup>, NO<sub>3</sub><sup>-</sup>, and NH<sub>4</sub><sup>+</sup> may be more sensitive to the cleaning procedures and the cleanliness of the melting system, rather than the quality of the DW. Previous work had shown that organic anions and NH<sub>4</sub><sup>+</sup> of ionic species are easily contaminated by laboratory equipment materials and operators' breathing.<sup>15,21</sup> Interestingly, NO<sub>3</sub><sup>-</sup> peaks were obvious in B-1 and B-2 but not in the instrumental blank. They may be caused by the HNO<sub>3</sub> that remained in the melting system after the cleaning procedures. Inclusions of the acidic fume emitted from the HNO<sub>3</sub> reagent in the clean room might also be possible during the DW soaking procedure of sample collection bottles for the ionic species.

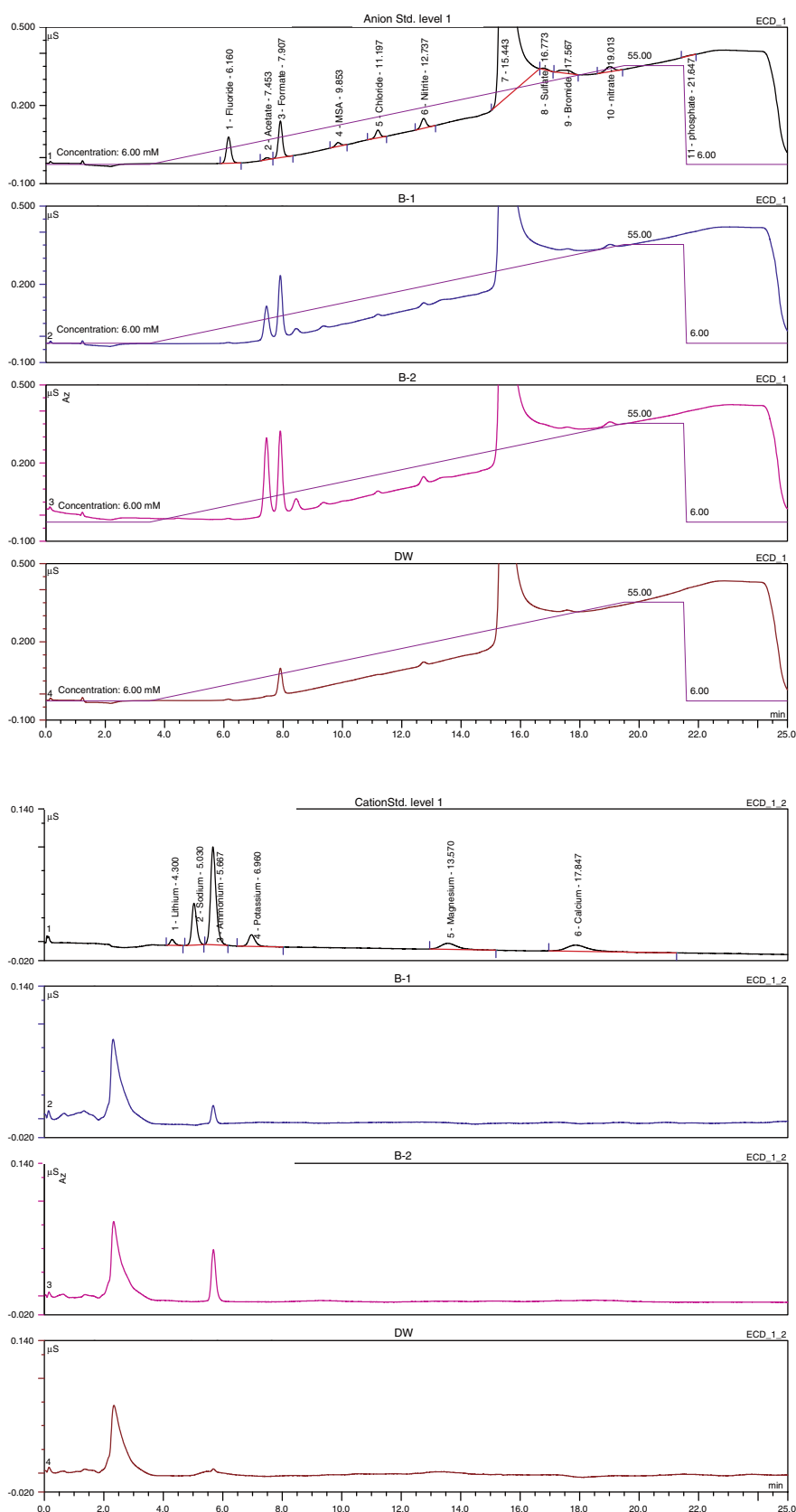
**Procedural Detection Limits and PB Levels.** The procedural detection limits (PDLs) and PBs were compared with previous results (Tables 3 and 4). The PDLs and PBs were determined for the melted sample from only the inner part of the blank ice core. The PBs were determined using a preconcentrated sample (~2 mL) because of the analytical errors caused by low levels of proxies in the melted blank ice-core sample.<sup>22</sup> They were generally higher than their PDLs by a factor of 2–3.

Table 3 shows that the PDLs of ionic species in the present study were comparable to the detection limit of continuous melting with a discrete sampling system (CMDS DL) reported by Osterberg *et al.*,<sup>12</sup> and the PBs were similar to those of Cole-Dai *et al.*,<sup>23</sup> except for NH<sub>4</sub><sup>+</sup>. The PB of NO<sub>3</sub><sup>-</sup> was

~2.00  $\mu$ g/L, which is the highest level for the ionic species. This is associated with NO<sub>3</sub><sup>-</sup> peaks in B-1 and B-2 explained in the previous subsection. However, the melting method established in this study might be useful for measuring Ca<sup>2+</sup> due to its PB which is roughly 10 times lower than those of other studies in Table 3 and to the lack of interference from the Ti melting head which shows no peaks at the near RT of Ca<sup>2+</sup> in the blank. Although peaks of NH<sub>4</sub><sup>+</sup> and organic anions were measurable in the system blank, their PDLs may still be superior to those of other studies.

Table 4 shows that the PDLs for Mn, Co, and Sr analyzed in this study were superior to the PBs of Knusel *et al.*,<sup>11</sup> but the PDLs for most elements were slightly higher than the CMDS DL reported by Osterberg *et al.*,<sup>12</sup> except for Mn and Cu. It is interesting to note that the PDL of Cu and Mn was superior to the CMDS DL of Osterberg *et al.*,<sup>12</sup> and the PDL of Pb was just roughly 2 times higher than CMDL DL of Osterberg and others. The system used in this study also provided meaningful measurements of Ni. This result highlights the advantages of a melting head made of Ti, as suggested by McConnell *et al.*<sup>10</sup> Among trace element species, the PB (90.0 ± 16.2 ng/L) for Zn indicated that the experimental procedures need to be refined in order to obtain valid Zn concentrations even though the melting head was made of Ti.

Finally, comparisons with previous results (Table S2) and PDLs of the melting system suggested that the melting system constructed in this study might successfully be



**Figure 3.** Chromatograms of ionic species in STD level 1, S-1, S-2, and DW (STD level 1:  $\text{Na}^+$ -0.40,  $\text{NH}_4^+$ -0.50,  $\text{K}^+$ -1.00,  $\text{Mg}^{2+}$ -0.50,  $\text{Ca}^{2+}$ -1.00,  $\text{F}^-$ -0.10,  $\text{CH}_3\text{CO}_2^-$ -0.49,  $\text{HCO}_2^-$ -0.49,  $\text{MSA}$ -0.50,  $\text{Cl}^-$ -0.51,  $\text{NO}_2^-$ -0.51,  $\text{SO}_4^{2-}$ -0.50,  $\text{Br}^-$ -0.50,  $\text{NO}_3^-$ -0.51  $\mu\text{g/L}$ . B-1: Blanks obtained by injecting DW filled in sample collection bottles. B-2: Blanks obtained by injecting DW to wash out the melting system).

applied to determine trace-element concentrations in ice-core samples drilled in Greenland and alpine areas (see Supporting Information).<sup>25–28</sup>

**Performance Tests: Decontamination Efficiency, Recovery Efficiency, and Memory Effect.** The decontamination efficiency of the melting system constructed in this study was systematically investigated. Figure 4 shows the ratios of the signal intensity of trace elements in the melted sample from the blank ice core and system blanks from the core surface toward its center. The system blank signal was used as a reference because it indicated the cleanliness of the melting system before melting of an ice-core sample. The results clearly indicate that the signal intensity ratios of elements in the melted sample from the inner part of the ice core approached unity, but that those in the melted sample from the middle and outer zones increased steadily. For Cu, Zn, Sr, Ba, and Pb, which are known to be easily contaminated in a laboratory environment, the signal intensity ratios in the

melted sample from the inner zone were slightly higher than unity, but their ratios with one standard deviation ( $1\sigma$ ) were approximately unity, which indicates no contamination of the melted sample from the inner zone. Figure 5 also shows the results of the ionic species in the melted sample from the blank ice core. They indicate that decontamination efficiencies of ions are similar to those of trace elements. The signal intensity ratios of most ionic species in melted samples from the inner part of the blank ice core were roughly unity, except for  $\text{NO}_3^-$ . This indicates that the melted sample from the inner part of the ice core remained free of contaminants except for  $\text{NO}_3^-$  during melting and that the levels of elements and ions should be determined with the melted sample from the inner part of the ice core.

The recovery efficiencies of trace elements in an ice core were investigated to determine whether element concentrations in the inner part of the core were preserved after the melting procedure. The concentrations of elements in artificial ice

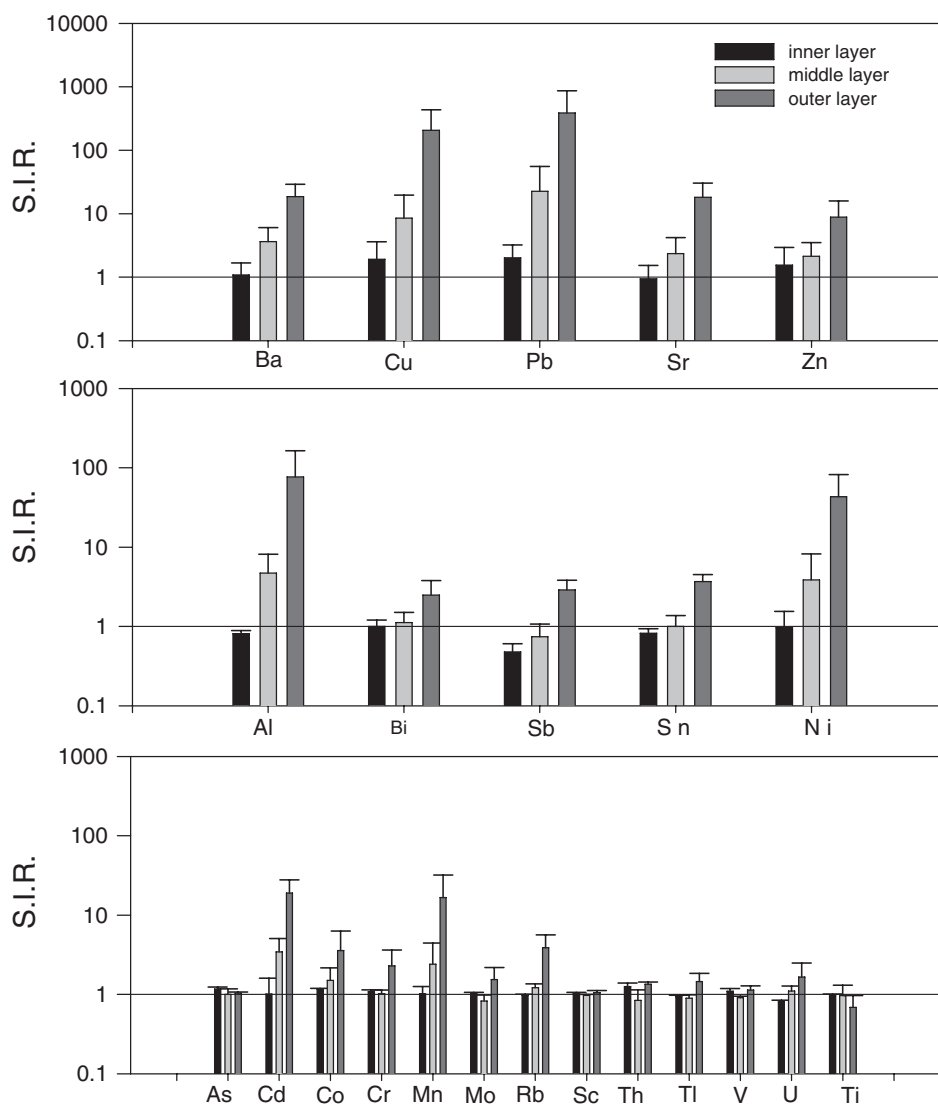


**Figure 4.** Signal intensity ratios (SIRs) of elements in blank artificial ice core to elements in system blank from three zones of the melting head during melting procedures. The ratio with 1 standard deviation is represented ( $n = 3$ ).



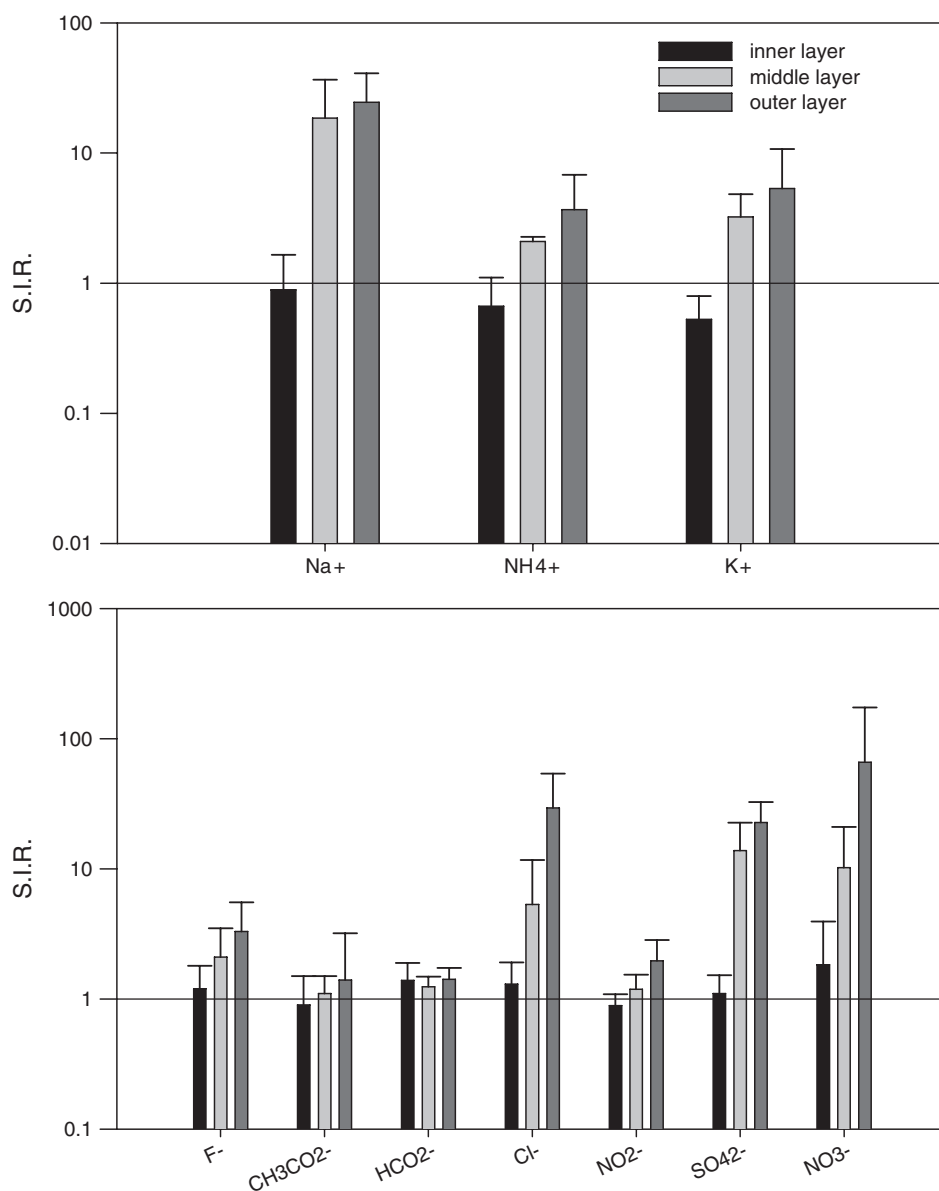


**Figure 5.** Signal intensity ratios (SIRs) of ionic species in blank artificial ice core to ionic species in system blank from three zones of melting head during melting procedures. The ratio with 1 standard deviation is represented ( $n > 5$ ).

cores processed by the melting system were compared with those of elements in an artificial ice core that was made at the same time, in order to calculate their recovery efficiencies (Figure 6). It is interesting to note that artificial ice cores are quite difficult to create such that the standard material contained within them is evenly distributed and the levels of elements in an artificial ice core can be contaminated during its preparation, such that they may differ from the levels of elements in the standard solution used to prepare the artificial ice core. In particular, concentrations of elements such as Cu, Zn, and Pb can differ markedly from the original levels in the standard solution, and their recoveries might then be overestimated if the concentration levels in standard solution are directly compared with theoretical levels.

The levels ( $\sim 100$  ng/L) of elements actually retained in artificial ice cores prepared under identical experimental conditions were compared as reference levels rather than element concentrations in the standard solution, which may remove the effects of contamination during preparation of artificial ice cores. The levels of elements in an artificial ice core were determined with melted samples, which were melted in a clean bottle (Nalgene, NA-2103-0032) in a class 10 laminar airflow booth in the clean laboratory (class 1000) at room temperature. The results of recovery efficiencies indicated that the first (Cr, As, Bi), second (V, Mn, Co, Ni, Rb, Sr, Cd, Sb), and third group (Cu, Zn, Pb) of elements were  $\sim 80\%$ ,  $\sim 90\text{--}100\%$ , and  $\sim 100\text{--}120\%$ , respectively (Figure 6). This shows that trace elements in ice cores can generally be extracted and

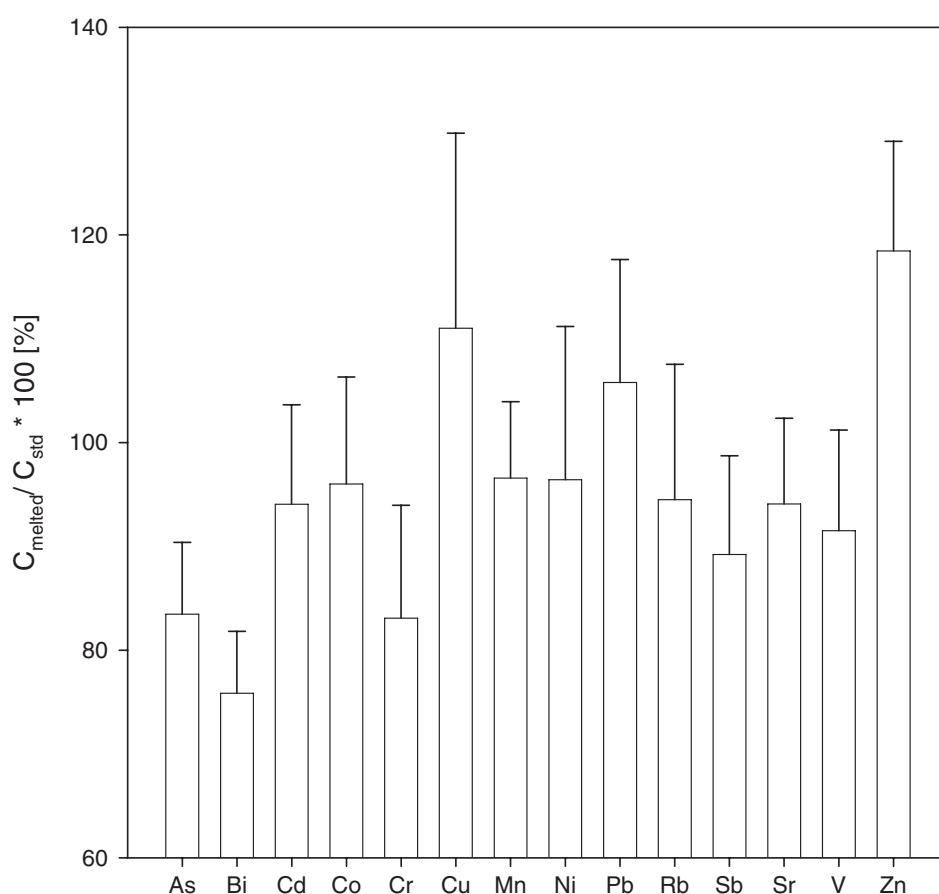


**Figure 6.** Recovery efficiencies of elements [ $n > 5$ ,  $C_{\text{melted}}$ : concentrations of elements of melted artificial ice core using the melting system,  $C_{\text{std}}$ : concentrations ( $\sim 100$  ng/L level except for Zn ( $\sim 170$  ng/L)) of elements of melted artificial ice core in an ultraclean 1 L Low-density polyethylene (LDPE) under a Class 10 laminar airflow booth in clean laboratory (class 1000)).

determined properly using the melting system constructed in this study.

The memory effects of elements in the melted sample on the melting system were investigated to determine the volume of DW needed to wash out the melting system. Figure 7 compares signal intensity ratios for elements in the rinsing DW and in the melted sample from the artificial ice core ( $\sim 100$  ng/L elements). Only the inner zone of the melting head was rinsed to test the memory effect of proxies in melted samples from the inner part of the ice core. In this study, the DW volume was limited to  $\sim 0.5$  mL per rinse due to the geometric design of the melting head. The results showed that V, Cr, Mn, Co, Ni, Cu, Zn, Rb, Sr, Cd, Sb, Pb, and Bi were totally cleaned with a rinse volume of  $\sim 1$ – $2$  mL, but more DW ( $\sim 3$  mL) was needed to wash out As. Interestingly, Cu, Zn, and Pb were likely to remain on the surface of the melting head and tubes after melting the ice-core samples, even though their uncertainties were larger than those of other elements. Considering the volume of DW to be used for rinsing and the time required for the total melting process, the melting system was designed to be rinsed with a total of  $\sim 2.5$  mL DW prior to each melting procedure in order to minimize the memory effects of trace elements between ice-core samples melted in series.

#### Preliminary Comparison of the Chiseling Method and Melting System.

The concentrations of trace elements obtained using the melting system were compared with those obtained using the manual decontamination method. As a test, an ice core from the East Rongbuk glacier on the northeast slope of Mount Everest ( $28^{\circ}03'N$ ,  $86^{\circ}96'E$ , 6518 m a.s.l.) was decontaminated by mechanical chiseling.<sup>29</sup> After the chiseling was complete, the inner core was either collected in whole or, if longer than 20 cm, was cut into several successive parts. During chiseling, both ends of each sample were held by plastic tumblers and remained uncut. These parts of the ice-core samples were decontaminated using the melting system, and both sample sets were analyzed for trace metals by the same ICP-MS.

Figure 8 shows the concentration variations of elements in ice-core samples decontaminated by the melting system and by the manual chiseling method. The results indicate that trace element concentrations in the ice-core samples treated by both methods were roughly comparable prior to AD  $\sim 1500$ , but did not compare well after AD  $\sim 1500$ . These differences may be due to the different time spans covered by each ice-core sample using two methods and chemical variability within the ice itself. Lee *et al.* have reported that concentrations of atmospheric trace elements at the drilling site showed large seasonal

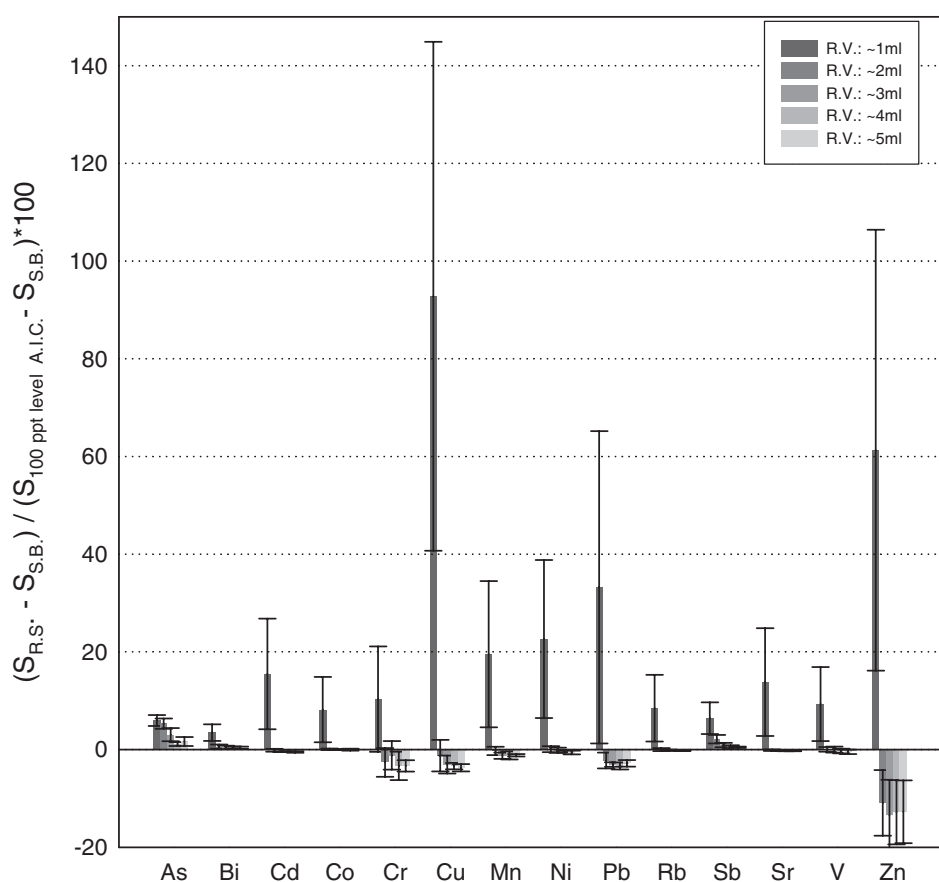


**Figure 7.** Memory effects of the melting system according to cumulative rinsing volume (RV) ( $S_{R.S.}$ : signal intensity of elements in liquid samples to wash out melting system in series,  $S_{S.B.}$ : signal intensity of elements in system blank,  $S_{100 \text{ ppt level A.I.C.}}$ : signal intensity of 100 ng/L artificial ice core,  $n = 3$ , Cu: ~200 ng/L, Pb: ~200 ng/L, Zn: ~300 ng/L, Others: ~100 ng/L).

variations between monsoon and non-monsoon seasons.<sup>17</sup> Considering that each sample treated by the melting system was 5 cm long and spanned <6 months after AD ~1500, trace element concentrations from the melted samples using the melting system may have been strongly affected by seasonal atmospheric conditions. However, this may be less significant in deeper samples prior to AD ~1500 because the deeper material is more compacted, and seasonal variations generally weaken with depth in an ice core. The 5-cm-long sample melted by the melting system prior to AD ~1500 in this study spanned ~1.4 years, which evened out the annual variations in trace element concentrations.<sup>17</sup> The same ice-core samples decontaminated by mechanical chiseling prior to AD ~1500 also spanned ~4.8 years. The measurement results of this period should therefore have been generally similar, even though the depth of ice core compared was not strictly identical.

### Conclusions

We have described the first research results of a Ti melting head in the melting system of ice cores, and reported on melting-system performance tests such as decontamination efficiency, recovery efficiency, and memory effects. The PDLs and PBs of ionic species and trace elements showed that

measurement of  $\text{NO}_3^-$  and Zn requires improved experimental procedures. Other ionic species and trace elements, such as  $\text{CH}_3\text{CO}_2^-$ ,  $\text{HCO}_2^-$ ,  $\text{NH}_4^+$ , Ni, Cu, and Pb, should also be carefully measured because they are easily influenced by DW purity and labware cleanliness, even in a clean laboratory environment.

Performance tests showed that ionic species and trace elements in the middle of an uncontaminated ice core can be measured using the melting system described in this study. The results also emphasize the importance of rigorous experimental procedures, from cleaning of labware to devices to collect the melted samples. The memory effects of trace elements show the importance of careful cleaning of the melting system before and after melting of ice-core samples in order to minimize interference between samples melted in series. In this study, short and discrete ice-core samples (5-cm-long ice core) were intentionally processed in the melting system, so that interference between melted samples could be minimized. The intercomparison results with a conventional chiseling method roughly validated the concentrations of trace elements determined by the melting system even though they were from only a few ice-core samples with similar depth intervals.

Based on PDLs and performance tests, the melting system with a Ti melting head, improved in this study, is expected to

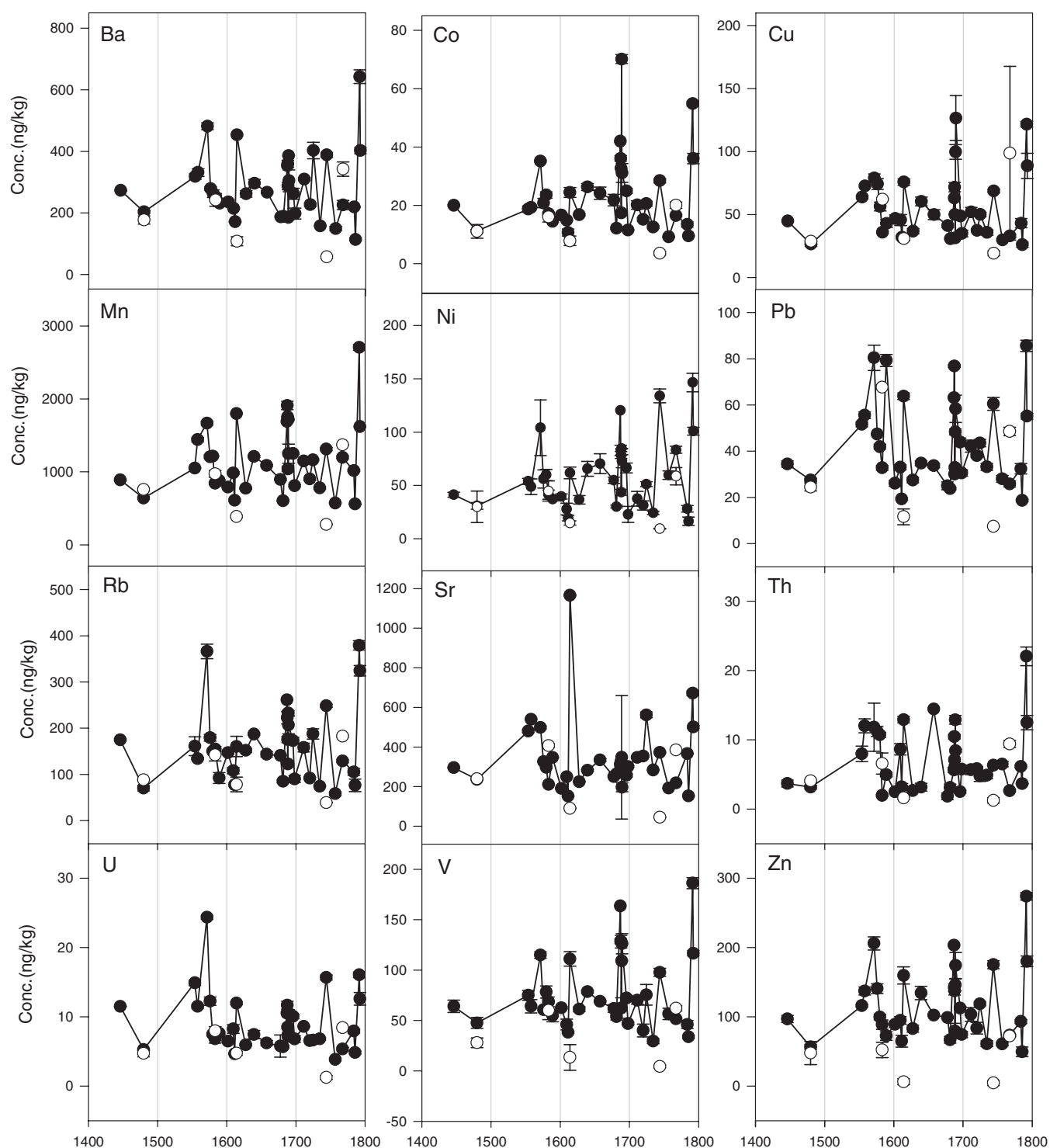


**Figure 8.** Intercomparisons between the manual decontamination method and the melting system from an ice core drilled at Mt. Everest (ice core sample: East Rongbuk (ER) glacier located on the northern slope of Mt. Everest, 28°03'N, 86°96'E, 6518 m a.s.l.) (Instrument: ICP-MS (Perkin Elmer Sciex, ELAN 6100), Errors given correspond to  $1\sigma$ , filled circle: manual decontamination method, empty circle: melting system)

be capable of successfully decontaminating ice-core samples from high-alpine areas as well as Greenland.

**Acknowledgments.** This work was supported by research grants (PE11090 and PE15010) from the Korean Polar

Research Institute. This research was also partly supported by the Basic Science Research Program through the National Research Foundation of Korea (NRF) funded by the Ministry of Education, Science and Technology (2012R1A1A2001832).



**Supporting Information.** Additional supporting information is available in the online version of this article.

### References

1. A. Ng, C. Patterson, *Geochim. Cosmochim. Acta* **1981**, *45*, 2109.
2. R. Delmas, *Rev. Geophys.* **1992**, *30*, 1.
3. M. Legrand, P. Mayewski, *Rev. Geophys.* **1997**, *35*, 219.
4. C. Boutron, C. Barbante, S. Hong, K. Rosman, M. Bolshov, F. Adams, P. Gabrielli, J. Plane, S. D. Hur, C. Ferrari, P. Cescon, In *Persistent Pollution – Past, Present and Future*, M. Quante, R. Ebinghaus, G. Flöser Eds., Springer-Verlag Berlin Heidelberg, 2011, p. 19.
5. W. Chisholm, K. Rosman, C. Boutron, J. P. Candelone, S. Hong, *Anal. Chim. Acta* **1995**, *311*, 141.
6. J. C. Priscu, E. E. Adams, W. B. Lyons, M. A. Voytek, D. W. Mogk, R. L. Brown, C. P. McKay, C. D. Takacs, K. A. Welch, J. D. Kirshtein, R. Avci, *Science* **1999**, *286*, 2141.
7. A. Sigg, K. Fuhrer, M. Anklin, T. Staffelbach, D. Zurmühle, *Environ. Sci. Technol.* **1994**, *28*, 204.
8. R. Rothlisberger, M. Bigler, M. Hutterli, S. Sommer, B. Stauffer, *Environ. Sci. Technol.* **2000**, *34*, 338.
9. T. M. Huber, M. Schwikowski, H. W. Gaggeler, *J. Chromatogr. A* **2001**, *920*, 193.
10. J. R. McConnell, G. W. Lamorey, S. W. Lambert, K. C. Taylor, *Environ. Sci. Technol.* **2002**, *36*, 7.
11. S. Knusel, D. E. Piguot, M. Schwikowski, H. W. Gaggeler, *Environ. Sci. Technol.* **2003**, *37*, 2267.
12. E. C. Osterberg, M. J. Handley, S. B. Sneed, P. A. Mayewski, K. J. Kreutz, *Environ. Sci. Technol.* **2006**, *40*, 3355.
13. P. R. Kaufmann, U. Federer, M. A. Hutterli, M. Bigler, S. Schupbach, U. Ruth, J. Schmitt, T. F. Stocker, *Environ. Sci. Technol.* **2008**, *42*, 8044.
14. M. Bigler, A. Svensson, E. Kettner, P. Vallelonga, M. E. Nielsen, J. P. Steffensen, *Environ. Sci. Technol.* **2011**, *45*, 4483.
15. T. Jauhianinen, J. Moore, P. Peramaki, J. Derome, K. Derome, *Anal. Chim. Acta* **1999**, *389*, 21.
16. D. Darbouret, I. Kano, *Millipore R&D Notebook RD002*, EMD Millipore, 1999, p. 1.
17. K. Lee, S. D. Hur, S. Hou, S. M. Hong, X. Qin, J. Ren, Y. Liu, K. Rosman, C. Barbante, C. Boutron, *Sci. Total Environ.* **2008**, *404*, 171.
18. S. B. Hong, W. H. Kim, H. J. Ko, S. B. Lee, D. E. Lee, C. H. Kang, *Atmos. Res.* **2011**, *101*, 427.
19. S. E. Tseren-Ochir, Y. S. Huh, S. Hong, H. J. Hwang, S. D. Huh, *Bull. Kor. Chem. Soc.* **2011**, *32*, 2105.
20. S. Hong, A. Liuberas, F. Rodriguez, *Korean J. Polar Res.* **2000**, *11*, 35.
21. Z. Genfa, P. K. Dasgupta, *Anal. Chem.* **1989**, *61*, 408.
22. U. Gorlach, C. Boutron, *Anal. Chim. Acta* **1990**, *236*, 391.
23. J. Cole-Dai, D. M. Budner, D. G. Ferris, *Environ. Sci. Technol.* **2006**, *40*, 6764.
24. A. Morganti, S. Becagli, E. Castellano, M. Severi, R. Traversi, R. Udisti, *Anal. Chim. Acta* **2007**, *603*, 190.
25. C. Barbante, M. Schwikowski, T. Doring, H. W. Gaggeler, U. Schotterer, L. Tobler, K. V. D. Velde, C. Ferrari, G. Cozzi, A. Turetta, K. Rosman, M. Bolshov, G. Capodaglio, P. Cescon, C. Boutron, *Environ. Sci. Technol.* **2004**, *38*, 4085.
26. L. Yuefang, Y. Tandong, W. Ninglian, L. Zhen, T. Lide, X. Baiging, W. Guangjian, *Ann. Glaciol.* **2006**, *43*, 154.
27. Y. Liu, S. Hou, S. Hong, S. D. Hur, K. Lee, Y. Wang, *J. Geophys. Res.* **2011**, *116*, D12307.
28. V. B. Aizen, P. A. Mayewski, E. M. Aizen, D. R. Joswiak, A. B. Surazakov, S. Kaspari, B. Grigholm, M. Krachler, M. Handley, A. Finaev, *J. Glaciol.* **2009**, *55*, 275.
29. S. Hong, K. Lee, S. Hou, S. D. Hur, J. Ren, L. Burn, K. Rosman, C. Barbante, C. Boutron, *Environ. Sci. Technol.* **2009**, *43*, 8060.